Quantum Electronics **48** (7) 589–595 (2018)

LASERS

https://doi.org/10.1070/QEL16705

Fibre-optic 100 fs pulse amplification and transmission system in the telecom range

A.A. Krylov, S.G. Sazonkin, A.F. Kosolapov, A.D. Pryamikov, A.N. Kolyadin, I.A. Bufetov

Abstract. **We have fabricated and investigated an efficient all-fibre source of ultrashort pulses of 100 fs duration with an energy of up to 5 nJ in the telecom range (near λ = 1.56 μm). Pulses from an erbium-doped fibre master oscillator with a minimum duration of 127 fs and repetition rate of 38.1 MHz were amplified in an erbium-doped active fibre to a maximum average power of 194.3 mW with a 30% efficiency under pumping by 640-mW single-mode laser diodes at a wavelength λ_{pump} = 976 nm and then compressed to an ~100 fs duration in a silica fibre with reduced nonlinearity (LMA fibre). The compressed pulses were launched with an efficiency over 80% into a hollow-core microstructured revolver fibre (HCRF) with a cladding formed by noncontacting cylindrical silica glass capillary tubes and a 61-μm-diameter hollow core. The measured loss for the fundamental mode of this fibre was under 30 dB km^{-1} at λ = 1.56 μm. Owing to the weak nonlinearity and low dispersion of the HCRF, output pulses were similar in characteristics (duration and spectrum) to input pulses even at HCRF lengths above 10 m.**

Keywords: *ultrashort pulse, erbium-doped fibre amplifier, pulse compression, self-phase modulation, group velocity dispersion, hollow-core fibre, pulse transmission.*

1. Introduction

Sources of ultrashort laser pulses (USPs) with a characteristic ultrabroad spectrum consisting of equidistant narrow lines (optical comb) find application in various areas of science, technology and medicine [1, 2]. Owing to the explosive growth of fibre-optic technologies, recent years have seen increasing use of USP sources based on erbium-doped active fibres, which emit ~100 fs pulses in the telecom range (near λ = 1.55 μm) [3, 4]. In particular, they are employed in ultrahigh-resolution molecular spectroscopy [2, 5, 6] and the optical frequency metrology of transitions in atoms and molecules [2, 7, 8]. Moreover, they are indispensable in designing optical frequency standards (optical clocks) [4, 8–12], as well as in multiphoton microscopy [13, 14], optical coherence tomography [15] and medicine [16]. Relatively recently, frequency-stabilised optical combs (referred to as astrocombs in the literature) began to be actively used to calibrate astronomical spectrographs in the search for exoplanets [2, 17] – planets whose characteristics are suitable for life.

It should be noted that most metrological applications of erbium-doped USP sources, including optical comb frequency stabilisation, involve the generation of a coherent optical supercontinuum with a spectral width above an octave [2, 8–12, 15, 17, 18]. Optimal pulses for these purposes have a duration of ~100 fs and average power of 100 mW or above (the energy of USPs with a centre wavelength of 1.55 μm then ranges from 1 to 10 nJ). Such pulses practically cannot be obtained directly from a master oscillator. In connection with this, it is necessary to amplify and then compress USPs from a master oscillator to obtain a high peak power sufficient for coherent spectral broadening in highly nonlinear optical fibres [8–12, 15, 18].

At present, there are two main approaches to the generation of ~100-fs USPs of ~10 nJ energy in the telecom range (the corresponding average power is 100 mW or above). They involve the amplification of pulses from an erbium-doped fibre laser oscillator but differ in the way final USPs are formed. Note that, in contrast to chirped pulse amplification [16, 19–21], a widely known method in which pulses are amplified after prestretching in order to significantly reduce the influence of nonlinear effects in the amplifier fibre, these two approaches take advantage of fibre nonlinearity for generating a coherent broad spectrum sufficient for producing ~100-fs USPs.

One approach is based on the soliton self-frequency shift (stimulated Raman self-scattering) to longer wavelengths in negative group velocity dispersion (GVD) fibres ($\beta_2 < 0$), an effect due to the delay of the nonlinear response of the medium and related to the imaginary part of the vibrational (molecular) third-order nonlinear susceptibility (and Raman gain in the medium) [22]. This leads to the formation of transform-limited fundamental solitons [so-called Raman solitons (RS's)] of ~100-fs duration with a centre wavelength of 1.6 μm or above [13, 14, 23, 24]. It is worth noting that RS's can be generated not only in passive fibres [13, 14, 24] but also directly in amplifier fibre [23], their particular parameters being determined to a large extent by the nonlinearity and GVD of the converter fibre. This effect can be used for USP 'normalisation', i.e. for the generation of transform-limited pedestal-free pulses without frequency modulation, which is extremely important for subsequent generation of few-cycle quality pulses [25]. Due to the limitation on the soliton energy (soliton theorem), the RS energy typically does not exceed 10 nJ [14, 23, 24]. Nevertheless, Horton et al. [13] demonstrated the generation of 65-fs RS's of 67 nJ energy at λ = 1675 nm, which seems to be a new record. The most promising application field of Raman solitons is

A.A. Krylov, A.F. Kosolapov, A.D. Pryamikov, A.N. Kolyadin, I.A. Bufetov Fiber Optics Research Center, Russian Academy of Sciences, ul. Vavilova 38, 119333 Moscow, Russia; e-mail: sokolak@mail.ru;
S.G. Sazonkin Bauman Moscow State Technical University, Vtoraya Baumanskaya ul. 5/1, 107005 Moscow, Russia

Received 17 April 2018
Kvantovaya Elektronika **48** (7) 589–595 (2018)
Translated by O.M. Tsarev

three-photon microscopy, where RS's at a wavelength near 1.7 μm are required [13, 14].

The other approach involves the nonlinear amplification of USPs in a positive-GVD erbium-doped active fibre ($\beta_2 > 0$) and subsequent pulse compression either using bulk dispersive elements (usually a prism pair [8, 9, 18, 24]) or in anomalous-GVD fibres owing to dispersion and soliton effects (multisoliton compression) [10, 11, 15, 25]. Note that normal GVD in an active fibre prevents pulse breakup in spite of the significant effect of self-phase modulation (SPM), which in turn compensates for the narrowing (filtering) of the spectrum on account of the limited gain bandwidth of the erbium-doped fibre (gain narrowing effect) [18]. Moreover, the combined effect of normal GVD and SPM in an active fibre produces a linear chirp of an amplified pulse throughout its length, which is extremely important for subsequent pulse compression [26].

A prism pair ensures good quality of compressed USPs (with no pedestal), but the configuration is then not all-fibre, which is an obvious drawback. Multisoliton compression in turn allows an all-fibre configuration to be retained, but because of the residual uncompensated chirp (due to the excess nonlinearity and higher order dispersion in the compressor fibre) the compressed pulses have an extended pedestal [27, 28], which can account for a considerable part (up to 60%) of the pulse energy [29].

Recently, Ferenbacher et al. [9] demonstrated 120-fs USPs with a record high average power of 600 mW (pulse energy of ~6 nJ) at $\lambda \approx 1560$ nm, compressed by a silicon prism pair, and Luo et al. [30] reported pulses of about 23 fs duration (about four light periods) and 120 mW average power (pulse energy of 2.8 nJ) in the case of multisoliton compression of 1-ps amplified pulses ($\lambda = 1560$ nm) in SMF-28 standard telecom fibre. The quality of compressed pulses can be improved, with an all-fibre configuration retained, by optimising the chirp of pulses entering an erbium-doped fibre amplifier [18, 25, 29–33] or utilising various multistage compression schemes with various types of fibre (including photonic crystal fibre) [10, 15, 25, 34, 35], which however leads to an undesirable decrease in USP energy due to splice losses. In this context, it is worth noting work by Nicholson et al. [31], who demonstrated high-quality 34 fs pulses of 8.7 nJ energy (average power of 400 mW) in the case of single-stage compression of amplified similaritons in a standard single-mode fibre.

Thus, the generation of high-quality ~100 fs USPs with an average power above 100 mW in an all-fibre configuration is an extremely topical issue that requires optimisation of the entire system: master oscillator, erbium-doped fibre amplifier and compressor fibre.

In this work, optimising the erbium-doped fibre amplifier and compressor fibre we have demonstrated efficient generation of about 100 fs high-quality USPs with an average power of up to 190.2 mW (energy of up to 5 nJ) at a centre wavelength of 1.56 μm. In addition, we have demonstrated USP transmission through a hollow-core revolver fibre longer than 10 m essentially without distortion and with a slight increase in pulse duration.

2. Experimental setup

Figure 1 shows a schematic of the experimental setup. Positively chirped 250-fs Gaussian pulses from an erbium-doped fibre master oscillator with a repetition rate of 38.1 MHz and $\lambda = 1560$ nm (average power of 9 mW) [36] were directed through an optical attenuator (OA) and fibre-optic isolator (ISO) to a 7-m length of positive-GVD erbium-doped active fibre, whose core was pumped by two single-mode laser diodes with a total power of 640 mW at a wavelength $\lambda_{pump} = 976$ nm using two fibre-optic wavelength-division multiplexers (980/1550 nm WDMs). The erbium-doped fibre, with a step-index profile ($\Delta n = 0.019$) and a core diameter of 3.8 μm, has an unsaturated absorption of 14 dB m^{-1} at a wavelength of 980 nm, which corresponds to the maximum of the $^4I_{15/2} \rightarrow {}^4I_{11/2}$ absorption band of Er^{3+} in a silica glass matrix, and a second order mode cutoff wavelength $\lambda_c = 1$ μm. Its mode field diameter (MFD) and GVD (β_2) measured at $\lambda = 1.56$ μm are 5.3 μm and +22.2 ps^2 km^{-1}, respectively.

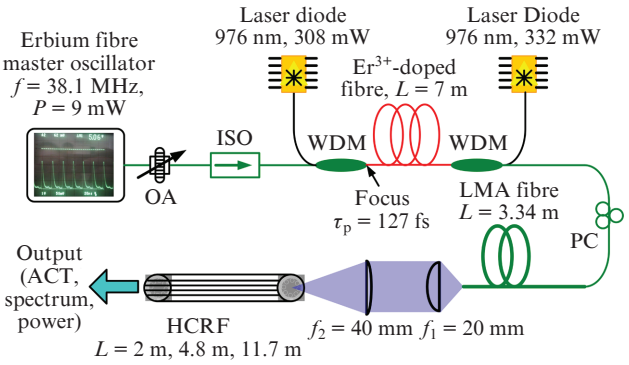

Figure 1. Schematic of the experimental setup (PC is a polarisation controller).

In our experiments, the length of the erbium-doped fibre was optimised so as to maximise the average output power of the amplified signal at the maximum pump power, which corresponded to the maximum slope efficiency of the amplifier. Along with the length of the active fibre, we optimised the magnitude and sign of the pulse chirp at the input of the erbium-doped fibre by placing SMF-28 standard fibre between the isolator and one of the WDMs. The position of the USP focus (the point where the USPs had the shortest duration, which was 127 fs in the case under consideration) proved to be optimal exactly at the input of the erbium-doped fibre (the distance from the output of the master oscillator to the erbium-doped fibre was 87 cm). Using the attenuator, the average power of the USPs at the output of the master oscillator was varied from 1 to 9 mW and, according to those experiments, the best results were obtained at an average output pulse power of 9 mW.

The amplified pulses were compressed in a large mode area (LMA) silica compressor fibre with a step-index profile ($\Delta n = 2.35\times10^{-3}$) and increased core diameter $D_{core} = 20\pm0.5$ μm, which was spliced directly to the WDM output. The calculated LP_{01} mode field diameter of the LMA fibre and GVD at $\lambda = 1.56$ μm were MFD = 18.3 μm and $\beta_2 = -28.9$ ps^2 km^{-1}. As shown below, increasing the mode field diameter of the compressor fibre leads to a considerable reduction in its nonlinearity coefficient, which eventually has an advantageous effect on the quality of the compressed pulses. The optimal length of the LMA fibre (L_{LMA}), corresponding to the minimum duration of the compressed USPs, was experimentally determined to be 3.34 m. It should be especially emphasised that the splice loss in the erbium-doped fibre + WDM + LMA fibre section was under 0.2 dB, which is unachievable in the case of pulse compression using bulk elements (e.g. prisms).

Using two plano-convex lenses with focal lengths f_1 = 20 mm and f_2 = 40 mm, the light from the angle cleaved end facet of the LMA fibre was launched with an efficiency of about 84% into a 30 cm diameter coiled hollow-core microstructured revolver fibre (HCRF) [37]. Figure 2a shows a cross-sectional scanning electron microscope image of the HCRF. The HCRF cladding is formed by eight noncontacting capillary tubes with a wall thickness of about 2.6 μm. The diameters of the hollow core and outer silica cladding are 61 and 153 μm, respectively, so that the calculated LP_{01} fundamental mode diameter is 45 μm.

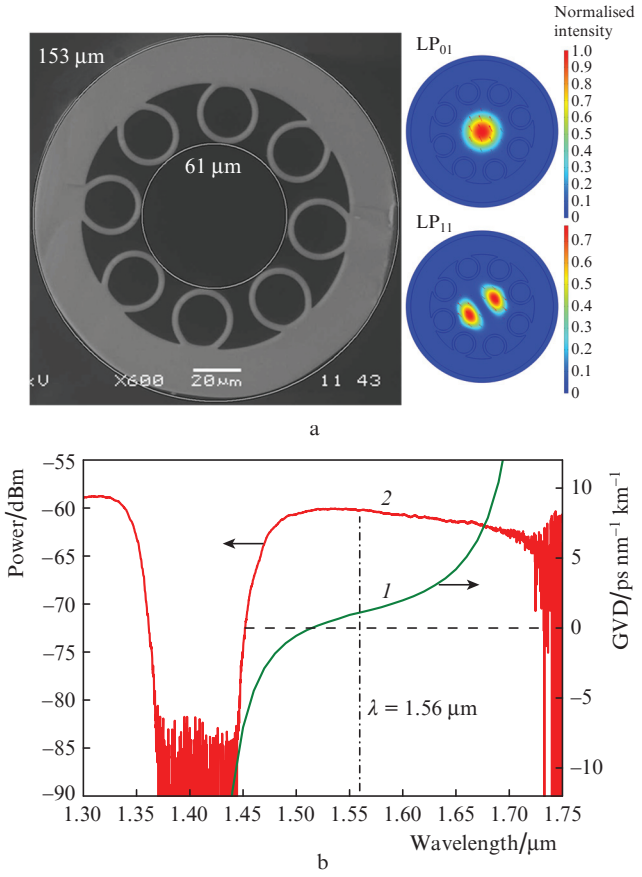

Figure 2. (Colour online) (a) Cross section of the HCRF and calculated profiles (intensity distributions) of its LP_{01} and LP_{11} modes; (b) (*1*) calculated GVD in the fundamental mode and (*2*) transmission spectrum of the HCRF.

Figure 2b shows the spectral dependence of the GVD calculated for the real structure of the fibre and the transmission spectrum of the HCRF under excitation with an Ocean Optics DH-2000 halogen lamp. It is seen that the spectral range of USP generation in the erbium-doped fibre laser oscillator falls in the third transmission zone of the HCRF (1.45–1.75 μm) according to the antiresonant reflecting optical waveguide (ARROW) model [38]. From Fig. 2b, we obtain for the LP_{01} fundamental mode $\beta_2 = -1.42$ ps^2 km^{-1} ($D = 1.1$ ps nm^{-1} km^{-1}) at $\lambda = 1.56$ μm, which is lower than the GVD of SMF-28 by more than one order of magnitude.

The measured loss in this fibre due to excitation of only the fundamental mode at $\lambda = 1560$ nm is about 27 dB km^{-1} [37], which is currently one of the best results for this type of hollow-core fibre.

Using parameters of the HCRF and the Kerr nonlinear refractive index of atmospheric air ($n_2 = 3\times10^{-23}$ m^2 W^{-1} [39]), we can estimate the nonlinearity coefficient γ of the fibre at a wavelength of 1.56 μm: $\gamma \approx 2\pi n_2/(\lambda A_{\text{eff}}) \approx 10^{-7}$ m^{-1} W^{-1}. This value is four orders of magnitude lower than the nonlinearity coefficient of SMF-28.

In our experiments, we measured pulse intensity autocorrelation traces (ACTs) using a Femtochrome autocorrelator with a scan range of 170 fs. Spectra of pulses were obtained using an ANDO spectrum analyser (0.6–1.75 μm) with a maximum resolution of 0.01 nm. The average output power was determined using an OPHIR power meter equipped with a thermopile sensor.

3. Experimental results

3.1. USP amplification and compression

Figure 3 shows intensity ACTs and spectra of amplified pulses at different pump power levels. We call attention to the fact that the measured ACTs are extremely well fitted by Gaussians (dashed line in Fig. 3a) despite the rather complex shape of the spectrum of the USPs, which is indirect evidence

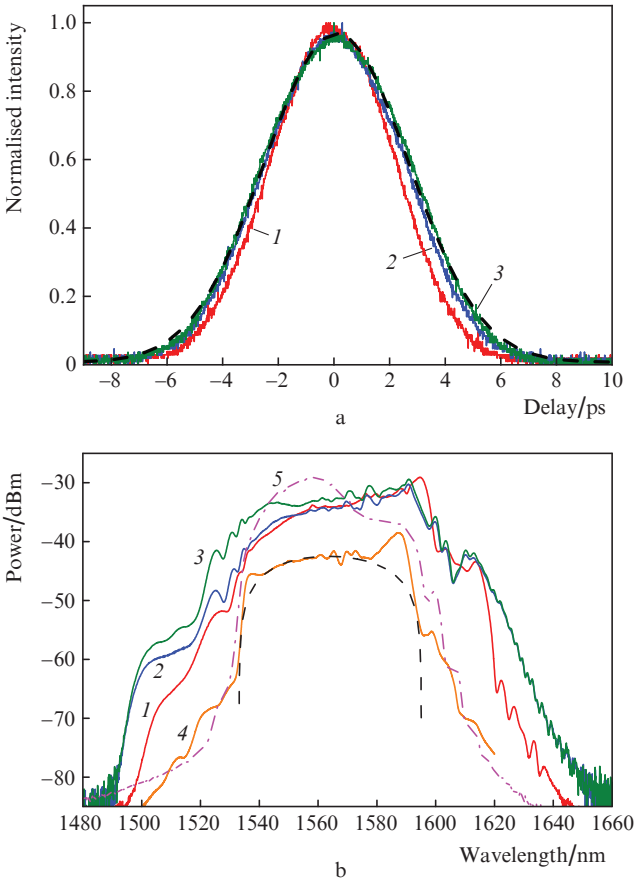

Figure 3. (a) Intensity ACTs and (b) spectra of (*1–3*) pulses at the output of the erbium-doped fibre amplifier, (*4*) pulses from the master oscillator at their focal point and (*5*) amplified chirped pulses. The dashed lines represent (a) a Gaussian and (b) parabola. (*1*) Pulse duration $\tau_p = 3.66$ ps, pulse energy $E_p = 2.7$ nJ, average power $P_{\text{out}}^{\text{av}} = 95$ mW; (*2*) $\tau_p = 4.12$ ps, $E_p = 4$ nJ, $P_{\text{out}}^{\text{av}} = 152.1$ mW; (*3*) $\tau_p = 4.33$ ps, $E_p = 5.1$ nJ, $P_{\text{out}}^{\text{av}} = 194.3$ mW; (*4*) $\tau_p = 127$ fs, $E_p = 0.2$ nJ, $P_{\text{out}}^{\text{av}} = 9$ mW; (*5*) $\tau_p = 50$ ps, $E_p = 2.9$ nJ, $P_{\text{out}}^{\text{av}} = 109$ mW.

of chirp linearity throughout the pulse. The USP duration rises from $\tau = 3.6$ ps at an average power at the amplifier output $P_{out}^{av} = 95$ mW to $\tau = 4.3$ ps at the maximum output power of 194.3 mW. Also shown in Fig. 3b is the spectrum of USPs from the master oscillator at their focal point (spectrum *4*), its best fit parabola (dashed line) [36] and the spectrum of chirped ~50 ps pulses (spectrum *5*) [37] amplified in the linear regime (with negligible nonlinear effects, including SPM, in the amplification process) in a 5-m length of the same erbium-doped fibre at an average signal output power of 109 mW. A marked narrowing (filtering) of the spectrum of USPs is well seen (to a 3 dB bandwidth of about 20 nm), due to the gain narrowing effect [18, 33] in the case of chirped pulse amplification. As a result, the compressed USP duration in the chirped pulse amplification configuration exceeds 300 fs [40]. On the other hand, nonlinear USP amplification demonstrated in this study ensures an essentially symmetric SPM-induced spectral broadening. Moreover, the combined effect of normal GVD and SPM in the fibre causes a larger pulse stretching in comparison with purely dispersion-induced broadening (nonlinear decompression) [26], as supported by experimental data (Fig. 3a). In addition, if the average power of pulses from the master oscillator was reduced (using the attenuator) to 1 mW at a constant pump power, the average signal power at the amplifier output dropped by about a factor of 1.5. The maximum duration of the amplified pulses was $\tau = 3.3$ ps and their spectrum was similar to the spectrum of USPs from the master oscillator.

To assess the quality of the amplified pulses and find out whether further pulse compression in the LMA fibre was worthwhile, the pulses were dechirped in a bulk compressor based on a pair of reflective diffraction gratings with a ruling density of 600 mm^{-1}. The diffraction efficiency of the gratings, η_d, was ~70%, and the total loss in the compressor, which comprised the gratings and two gold mirrors, was about 5 dB. The negative GVD introduced by the compressor was evaluated to be –2.4 ps^2 m^{-1}. Figure 4 shows the intensity ACT obtained at the shortest compressed pulse duration τ_p^{DG} = 176 fs and the highest amplifier pump power and corresponding to the optimum grating separation of 18 mm. It was measured together with the intensity ACT of pulses from the master oscillator at the focal point (τ_p^{MO} = 127 fs). It is seen that the two pulse durations differ somewhat (by about a factor of 1.4). Moreover, the compressed pulse ACT has small wings, attributable to the uncompensated SPM-induced nonlinear chirp and the effect of the third-order dispersion in the amplifier and grating compressor, which is particularly important in the case of the broad spectrum of USPs in Fig. 3b [25, 27, 41]. At the same time, the pulse compressed in the grating compressor has no extended pedestal. This strongly suggests that, despite the rather complex shape of their spectrum, the amplified pulses are linearly chirped even at the highest output power of 194.3 mW. It should be noted that the use of a compressor based on volume diffraction gratings is not an optimal approach for compressing chirped ~10 ps pulses obtained in a nonlinear amplification scheme.

Figure 5 shows the intensity ACTs and spectra of pulses compressed in the LMA fibre. The pulse duration varies in the narrow range 99–110 fs, depending on pulse energy, which is about a factor of 1.8 less than the duration of pulses compressed by the grating compressor (τ_p^{DG} = 176 fs). This means that the dispersion-induced pulse dechirping in the

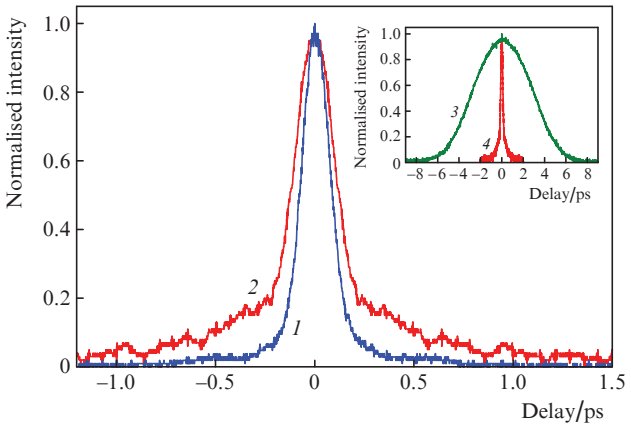

Figure 4. Intensity ACTs of (*1*) pulses from the master oscillator at their focal point and (*2*) pulses compressed by the grating compressor. Inset: intensity ACTs of (*3*) amplified pulses and (*4*) pulses compressed by the grating compressor. (*1*) Pulse duration τ_p = 127 fs, average power P_{out}^{av} = 9 mW; (*2*, *4*) τ_p = 176 fs, P_{out}^{av} = 57 mW; (*3*) τ_p = 4.33 ps, P_{out}^{av} = 194.3 mW.

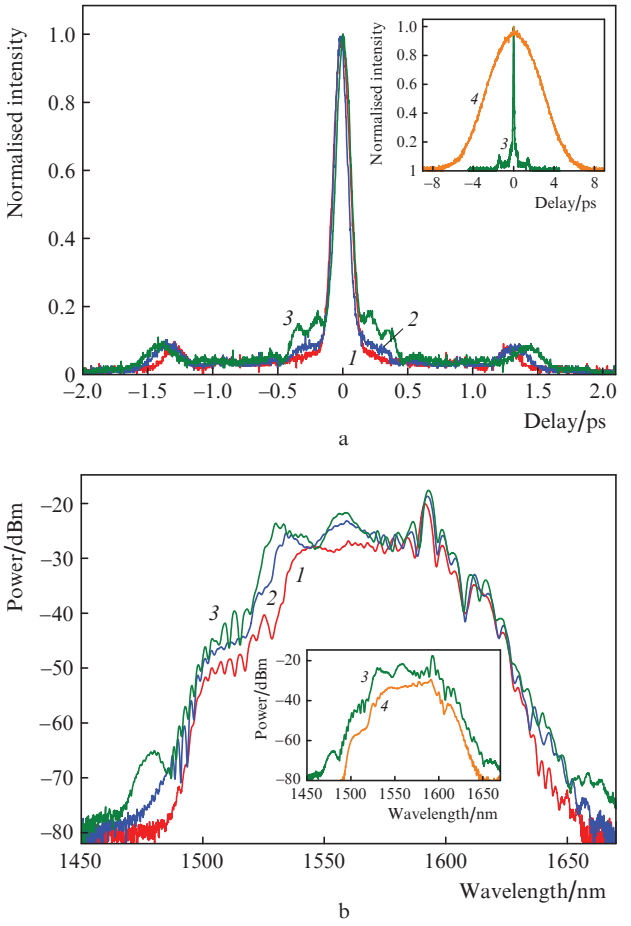

Figure 5. (a) Intensity ACTs and (b) spectra of pulses at the output of the (*1*–*3*) LMA fibre and (*4*) erbium-doped fibre amplifier at the following parameters: (*1*) pulse duration τ_p = 110 fs, pulse energy E_p = 2.4 nJ, average power P_{out}^{av} = 90.7 mW; (*2*) τ_p = 99 fs, E_p = 3.9 nJ, P_{out}^{av} = 147.2 mW; (*3*) τ_p = 101 fs, E_p = 5 nJ, P_{out}^{av} = 190.2 mW; (*4*) τ_p = 4.33 ps, E_p = 5.1 nJ, P_{out}^{av} = 194.3 mW.

LMA fibre was accompanied by further pulse compression due to soliton effects (multisoliton compression) [27,28]. Note that, because of the weaker nonlinearity of the LMA fibre, these effects were only significant at USP durations $\tau_p < 1$ ps, where the peak pulse power reached the SPM threshold. Indeed, the excessive effect of SPM is evidenced by the additional modulation in the spectrum of compressed USPs (Fig. 5b) [22] and the characteristic pedestal in the ACT of compressed pulses [27]. From $\tau_p^{DG}/\tau_p^{LMA} \sim 1$ and multisoliton compression theory [27,28], the equivalent order of the initial, transform-limited soliton can be estimated in this case at $N_0 \sim 1$. Owing to this, the quality of compressed pulses, which is evaluated as the fraction of energy in the central compressed peak, should be substantially higher than that for $N_0 \gg 1$ [42]. Moreover, reducing the nonlinearity of the compressor fibre, γ, also helps reduce the equivalent soliton order N_0, which has an advantageous effect on the quality of compressed USPs. In particular, the central peak in their ACT accounts for $\delta \approx 50\%$ of the energy even at the maximum average power of compressed pulses, $P_{out}^{av} = 190.2$ mW ($\delta \approx 60\%$ at $P_{out}^{av} = 90.7$ mW), which is markedly better than the quality of pulses compressed in standard fibre (SMF-28) at $N_0 \gg 1$ [27, 28, 42]. The maximum peak power of compressed pulses then reaches 23 kW.

Note also that the compressed pulse duration is essentially independent of pulse energy (average output power), as is the soliton order, which was calculated to be $N \approx 1$. Therefore, like in the case of Raman solitons, the parameters of a pulse compressed using soliton effects in fibre (multisoliton compression) correspond to a fundamental soliton, i.e. $N = 1$ is the ultimate compression condition [42]. Moreover, the minimum compressed pulse duration in this case scales as $\tau_p \propto \sqrt{|\beta_2|/\gamma}$ [28]. Thus, to reduce the compressed pulse duration, one should use a compressor fibre with lower GVD and stronger nonlinearity, e.g. a dispersion-shifted fibre (as in a number of previous studies [34,35,43]). It is for this reason that high-quality few-cycle pulses ($\tau_p \approx 20$ fs) are generated using two-step compression, with highly nonlinear dispersion-shifted fibres employed in the final step [34,43].

Figure 6 shows the average USP power at the amplifier and compressor fibre outputs as a function of diode pump power. The slope efficiency of the entire system is $\eta = 30.2 \pm 0.3\%$,

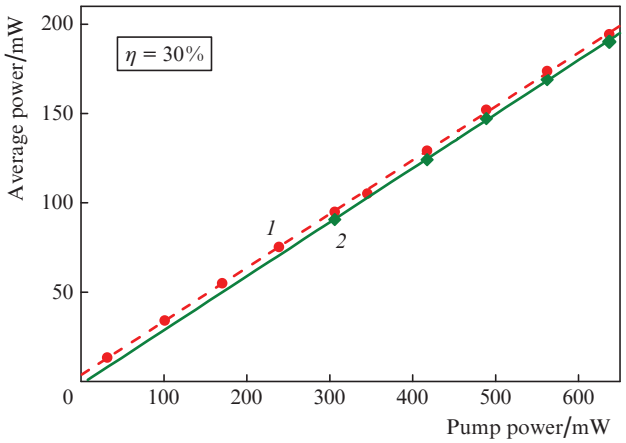

Figure 6. Average output power of the (*1*) erbium-doped fibre amplifier and (*2*) LMA fibre as a function of diode pump power at a wavelength of 976 nm.

which is one of the best results in the world for single-mode pumping at $\lambda_{pump} = 980$ nm [8, 11, 15, 18, 30, 32, 33].

3.2. USP transmission through the HCRF

We studied the transmission of compressed USPs over 2, 4.8 and 11.7 m lengths of the HCRF. Figure 7a shows the spectrum of USPs at the output of the 11.7-m-long HCRF (at the maximum input pulse energy) and the initial spectrum of the compressed pulses. It is seen that the spectrum at the HCRF output is essentially identical in shape to the initial spectrum, which is quite natural given the weak nonlinearity of the HCRF, filled with atmospheric air. Indeed, the calculated soliton order for pulses entering the HCRF is $N < 0.1$. The nonlinear length then exceeds 500 m even for USPs with the maximum energy. Thus, USP propagation through the HCRF is purely dispersive [44]. Figure 7b shows the USP duration at the output of the HCRF as a function of its length L at different input pulse energies. It is seen that the initial pulse duration (about 100 fs) increases by just 30% as a result of pulse propagation through the 11.7-m-long HCRF. Moreover, the pulse duration increases monotonically with increasing HCRF length. Note that fitting the experimental data with a

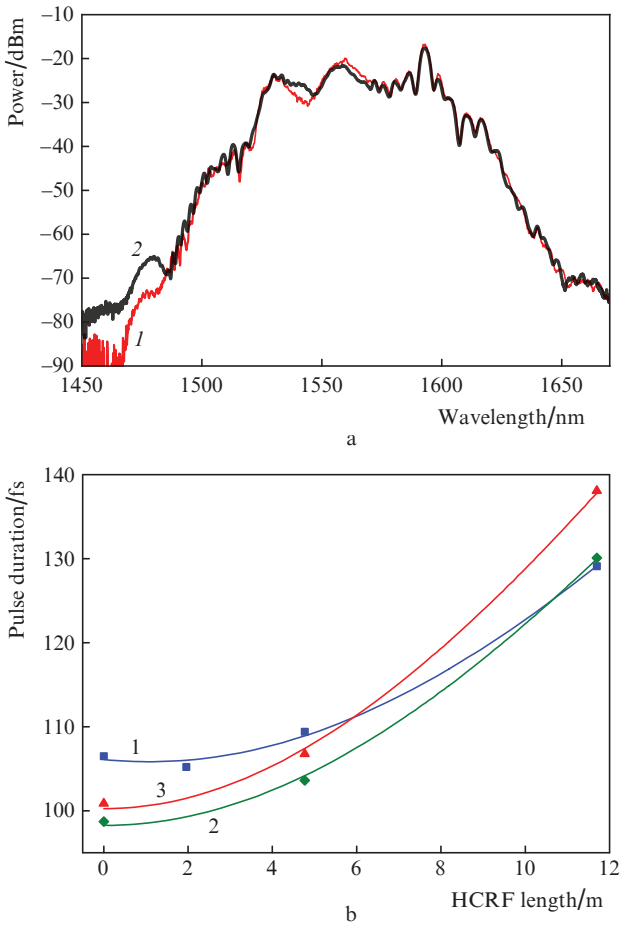

Figure 7. (a) Spectra of pulses at the outputs of the (*1*) HCRF and (*2*) LMA fibre at the highest erbium fibre amplifier pump power and (b) evolution of the compressed pulse duration in the HCRF at different input pulse energies: (*1*) $E_p = 3.3$ nJ, $P_{out}^{av} = 124.2$ mW; (*2*) $E_p = 3.9$ nJ, $P_{out}^{av} = 147.2$ mW; (*3*) $E_p = 4.4$ nJ, $P_{out}^{av} = 169$ mW.

function corresponding to the evolution of a chirped Gaussian pulse [22],

$$\tau_{\rm p} = \tau_{\rm p}^{\rm min}\sqrt{1+\left(\frac{C(L-L_0)}{L_{\rm D}}\right)^2+\left(\frac{L-L_0}{L_{\rm D}}\right)^2} \qquad (1)$$

(where $\tau_{\rm p}^{\rm min}$ is the dechirped pulse duration at point L_0; $C = (\partial^2\varphi/\partial t^2)(\tau_{\rm p}^2/(4\ln 2))$ is a dimensionless chirp; and $L_{\rm D} = (1/(4\ln 2))((\tau_{\rm p}^0)^2/|\beta_2|)$ is the dispersion length of the initial Gaussian pulse of duration $\tau_{\rm p}^0$), yields $C \approx 0$ at $L_0 \approx 0$ in all cases (which also confirms that compressed pulses have no linear chirp) and a dispersion length in the HCRF $L_{\rm D} \approx 15$ m. This value of $L_{\rm D}$ can be used to estimate the effective GVD β_2 in the hollow-core fibre: $|\beta_2| \approx 0.27$ ps^2 km^{-1}. This corresponds to a dispersion parameter $|D| \approx 0.21$ ps nm^{-1} km^{-1}. Since it is impossible to neglect the variation of the GVD in the hollow-core fibre over the entire spectrum of compressed USPs (i.e. the effect of the third-order dispersion in the HCRF should be taken into account), this estimate is slightly below the actual GVD in the hollow-core fibre at a wavelength of 1.56 μm.

4. Conclusions

We have demonstrated a fibre-optic system for the nonlinear amplification of ultrashort (100 fs) pulses in the telecom range, which comprises an erbium-doped fibre master oscillator, a USP amplifier based on a positive-GVD erbium-doped fibre and a negative-GVD compressor fibre with an increased mode diameter (LMA fibre). Optimisation of the system has ensured efficient generation of 100-fs high-quality USPs with an average power of up to 190.2 mW (energy of up to 5 nJ; pulse pedestal accounting for less than 50% of the energy) at a centre wavelength of 1.56 μm. We have demonstrated low-loss (< 30 dB km^{-1}) USP transmission through a hollow-core revolver fibre with negligible distortion and a slight increase (under 30%) in pulse duration at fibre lengths of ~10 m. According to an estimate based on experimental data, quality USP transmission [with an increase in USP duration by no more than a factor of 2 (to 200 fs)] is possible at HCRF lengths of up to 26 m.

The proposed USP source can be used for efficient second harmonic and coherent optical supercontinuum generation and in related applications, including those requiring efficient USP delivery with no significant distortion.

Acknowledgements. We are deeply grateful to M.E. Likhachev [Fiber Optics Research Center, Russian Academy of Sciences (RAS)] for providing the erbium-doped and LMA fibres and to A.K. Senatorov for measuring the GVD in the fibres. We are also indebted to B.L. Davydov [Institute of Radio Engineering and Electronics (Fryazino Branch), RAS] and R.R. Kharisov (Moscow Institute of Physics and Technology) for technical assistance.

References

1. Fermann M.E., Galvanauskas A., Sucha G. *Ultrafast Lasers: Technology and Applications* (New York: Marcel Dekker, 2001).
2. Diddams S.A. *J. Opt. Soc. Am. B*, **27**, B51 (2010).
3. http://avesta.ru/products/lasers/femtosekundnie-volokonnie-laseri/
4. http://www.menlosystems.de/
5. Coddington I., Newbury N., Swann W. *Optica*, **3**, 414 (2016).
6. Imrul Kayes M., Rochette M. *Opt. Lett.*, **43**, 967 (2018).
7. Udem Th., Holzwarth R., Hänsch T.W. *Nature*, **416**, 233 (2002).
8. Adler F., Moutzouris K., Leitenstorfer A., Schnatz H., Lipphardt B., Grosche G., Tauser F. *Opt. Express*, **12**, 5872 (2004).
9. Fehrenbacher D., Sulzer P., Liehl A., Kalberer T., Riek C., Seletskiy D.V., Leitenstorfer A. *Optica*, **2**, 917 (2015).
10. Lim J., Knabe K., Tillman K.A., Neely W., Wang Y., Amezcua-Correa R., Couny F., Light P.S., Benabid F., Knight J.C., Corwin K.L., Nicholson J.W., Washburn B.R. *Opt. Express*, **17**, 14115 (2009).
11. Kuse N., Jiang J., Lee C.-C., Schibli T.R., Fermann M.E. *Opt. Express*, **24**, 3095 (2016).
12. Nyushkov B.N., Pivtsov V.S., Kolyada N.A., Kaplun A.B., Meshalkin A.B. *Quantum Electron.*, **45**, 486 (2015) [*Kvantovaya Elektron.*, **45**, 486 (2015)].
13. Horton N.G., Wang K., Kobat D., Clark C.G., Wise F.W., Schaffer C.B., Xu C. *Nat. Photonics*, **7**, 205 (2013).
14. Cadroas P., Abdeladim L., Kotov L., Likhachev M., Lipatov D., Gaponov D., Hideur A., Tang M., Livet J., Supatto W., Beaurepaire E., Février S. *J. Opt.*, **19**, 065506 (2017).
15. Nomura Y., Kawagoe H., Hattori Y., Yamanaka M., Omoda E., Kataura H., Sakakibara Y., Nishizawa N. *Appl. Phys. Express*, **7**, 122703 (2014).
16. Morin F., Druon F., Hanna M., Georges P. *Proc. SPIE*, **7580**, 75800T (2010).
17. McCracken R.A., Charsley J.M., Reid D.T. *Opt. Express*, **25**, 15058 (2017).
18. Tauser F., Leitenstorfer A., Zinth W. *Opt. Express*, **11**, 594 (2003).
19. Galvanauskas A. *IEEE J. Sel. Top. Quantum Electron.*, **7**, 504 (2001).
20. Sobon G., Kaczmarek P.R., Sliwinska D., Sotor J., Abramski K.M. *IEEE J. Sel. Top. Quantum Electron.*, **20**, 3100205 (2014).
21. Peng X., Kim K., Mielke M., Jennings S., Masor G., Stohl D., Chavez-Pirson A., Nguyen D.T., Rhonehouse D., Zong J., Churin D., Peyghambarian N. *Opt. Express*, **22**, 2459 (2014).
22. Agrawal G.P. *Nonlinear Fiber Optics* (Oxford: Academic Press, 2013).
23. Nicholson J.W., Desantolo A., Kaenders W., Zach A. *Opt. Express*, **24**, 23396 (2016).
24. Tauser F., Adler F., Leitenstorfer A. *Opt. Lett.*, **29**, 516 (2004).
25. Takayanagi J., Nishizawa N., Sugiura T., Yoshida M., Goto T. *IEEE J. Quantum Electron.*, **42**, 287 (2006).
26. Tamura K., Nakazawa M. *Opt. Lett.*, **21**, 68 (1996).
27. Chan K.C., Liu H.F. *IEEE J. Quantum Electron.*, **31**, 2226 (1995).
28. Chen C.-M., Kelley P.L. *J. Opt. Soc. Am. B*, **19**, 1961 (2002).
29. Lin G.-R., Lin Y.-T., Lee C.-K. *Opt. Express*, **15**, 2993 (2007).
30. Luo H., Zhan L., Zhang L., Wang Z., Gao C., Fang X. *J. Lightwave Technol.*, **35**, 3780 (2017).
31. Nicholson J.W., Yablon A.D., Westbrook P.S., Feder K.S., Yan M.F. *Opt. Express*, **12**, 3025 (2004).
32. Purdie D.G., Popa D., Wittwer V.J., Jiang Z., Bonacchini G., Torrisi F., Milana S., Lidorikis E., Ferrari A.C. *Appl. Phys. Lett.*, **106**, 253101 (2015).
33. Sun J., Zhou Y., Dai Y., Li J., Yin F., Dai J., Xu K. *Appl. Opt.*, **57**, 1492 (2018).
34. Kibler B., Billet C., Lacourt P.-A., Ferriere R., Dudley J.M. *IEEE Photonics Technol. Lett.*, **18**, 1831 (2006).
35. Lin Y.-T., Lin G.-R. *Opt. Lett.*, **31**, 1382 (2006).
36. Krylov A.A., Sazonkin S.G., Lazarev V.A., Dvoretskiy D.A., Leonov S.O., Pnev A.B., Karasik V.E., Grebenyukov V.V., Pozharov A.S., Obraztsova E.D., Dianov E.M. *Laser Phys. Lett.*, **12**, 065001 (2015).
37. Krylov A.A., Senatorov A.K., Pryamikov A.D., Kosolapov A.F., Kolyadin A.N., Alagashev G.K., Gladyshev A.V., Bufetov I.A. *Laser Phys. Lett.*, **14**, 035104 (2017).
38. Litchinitser N.M., Abeeluck A.K., Headley C., Eggleton B.J. *Opt. Lett.*, **27**, 1592 (2002).
39. Nibbering E.T.J., Grillon G., Franco M.A., Prade B.S., Mysyrowicz A. *J. Opt. Soc. Am. B*, **14**, 650 (1997).
40. Chung H.-Y., Liu W., Cao Q., Kartner F.X., Chang G. *Opt. Express*, **25**, 15760 (2017).

41. Haus H.A., Moores J.D., Nelson L.E. *Opt. Lett*., **18**, 51 (1993).
42. Krylov A.A., Chernysheva M.A., Chernykh D.S., Kryukov P.G., Dianov E.M. *Laser Phys*., **23**, 075107 (2013).
43. Anashkina E.A., Andrianov A.V., Muravyev S.V., Kim A.V. *Opt. Express*, **19**, 20141 (2011).
44. Yatsenko Yu.P., Krylov A.A., Pryamikov A.D., Kosolapov A.F., Kolyadin A.N., Gladyshev A.V., Bufetov I.A. *Quantum Electron*., **46**, 617 (2016) [*Kvantovaya Elektron*., **46**, 617 (2016)].